Seismic vulnerability assessment of existing school buildings

SEISMIC VULNERABILITY ASSESSMENT OF EXISTING SCHOOL BUILDINGS

Marco Domaneschi [1*], Ali Zamani Noori [2], Maria Vittoria Pietropinto[3], and Gian Paolo Cimellaro [4]

ABSTRACT

This paper presents a methodology to perform the seismic vulnerability assessment of existing buildings. It starts with the acquisition of structural data from available construction drawings and field investigations to create a preliminary finite element model. Then, a wireless sensor network is used to collect the structural response at different locations. The sensors are connected and synchronized to each other to download and process data in real time. Modal identification methods, such as output-only and forced vibration techniques, are used to determine the modal characteristics and consequently calibrate the structural model for the subsequent vulnerability assessment. The proposed methodology is applied to a reinforced concrete school building in Italy. The seismic vulnerability is evaluated using a variety of alternative formulations. In particular, material nonlinearities and contact interaction at the structural joints are considered.

Keywords: Seismic vulnerability; wireless sensors; dynamic characterization; model calibration; existing school buildings

[1*] *Corresponding author: Assistant Professor, Department of Structural, Geotechnical and Building Engineering, Politecnico di Torino, Italy, E-mail: marco.domaneschi@polito.it.*

[2] *Postdoctoral research associate, Department of Structural, Geotechnical and Building Engineering, Politecnico di Torino, Italy, E-mail: ali.zamani@polito.it..*

[3] *Research assistant, Department of Structural, Geotechnical and Building Engineering, Politecnico di Torino, Italy, E-mail: mavi.pietropinto@gmail.com*

[4] *Professor, Department of Structural, Geotechnical and Building Engineering, Politecnico di Torino, Italy, E-mail: gianpaolo.cimellaro@polito.it.*

1. INTRODUCTION

Strong earthquakes affecting urban areas may have disastrous consequences where buildings have been designed without appropriate seismic codes. This is even more critical when it comes to national heritage and strategic buildings such as schools. As an example, the Italian school building asset consists of more than 47,000 structures, of which 60% were built before the introduction of the technical regulations on school building [1] and before the settlement of special requirements standards for seismic areas [2]. Despite 50% of school buildings on the Italian territory are located in earthquake affected areas with a medium-high hazard level, statistics show that 10% were built according to seismic safety criteria and 48% have a static load certification [3].

Current Italian standard [4] requires the evaluation of the seismic vulnerability index for existing structures through the assessment of the maximum bearing capacity. With respect to previous codes, where the attention was focused on the structural verification to withstand an assigned level of seismic demand, the Italian standard [4] follows the concept of the capacity function based on performance based seismic engineering framework [5]. Similar requirements were previously introduced in the Italian regulation for dams [6], moving the problem from the seismic hazard characterization at site level to the structural fragility [7].

The seismic vulnerability of an existing structure depends on several key components and it can be described as its susceptibility to damage by ground shaking of a given intensity. The aim of the seismic vulnerability assessment is to obtain the probability of a given damage level due to an earthquake scenario. As design data, it requires information such as the quality of the constitutive materials, the building age, the level of maintenance etc., which may not be available and, therefore, should be collected through inspections and surveys.

Different methods have been proposed for vulnerability assessment that can be divided into two main categories: *empirical* or *analytical*. However, both can be used together as a *hybrid* method [8, 9]. *Empirical* methods allow evaluating the seismic vulnerability by correlating the seismic intensity with the level of damage observed (statistical approach). This requires damage data from past earthquakes which may not be always available and cannot be used to assess the vulnerability of an individual building. There are two main types of empirical methods: (i) a discrete form of the conditional probability of obtaining a certain damage level due to a certain ground motion (damage probability matrices) and (ii) vulnerability functions expressing the probability to exceed a given damage state, given a function of an earthquake intensity.

On the other hand, *mechanical* approaches use *analytical* models that reproduce the main characteristics of buildings and estimate the capacity of the structure with respect to the demand level imposed by the earthquake scenario (quantitative approach). This method requires detailed knowledge of building including the real geometric characteristics and the current mechanical properties of the structure through the definition and calibration of appropriate calculation models. Depending on the type of structure and the degree of accuracy required, several types of analyses can be conducted to assess the seismic capacity of structure [10-16].

Combination of *empirical* and *mechanical* approaches belongs to the *hybrid* model for seismic vulnerability assessment. It can be particularly advantageous when there is a lack of damage data at a certain intensity level for the considered geographical area. Hybrid models allow calibration of the analytical model to be carried out. Besides, observational data may reduce computational efforts that would be required to produce a complete set of analytical vulnerability curves.

Among the experiences of seismic vulnerability assessment for existing building, Asteris, Chronopoulos [17] presented a methodology for earthquake resistant design or assessment of masonry structural systems. They tested the entire process using case studies from historical masonry structures in the European area,

namely Greece, Portugal and Cyprus. The seismic vulnerability assessment of a historic masonry building in Central Italy after the 2012 seismic events (May 20th and 29th) are reported by Formisano and Marzo [18] using a simplified approach given by Italian Guidelines on Cultural Heritage. In Di Lorenzo, Formisano [19], the seismic behavior of a masonry church was investigated through a two-steps approach. It consisted in a preliminary experimental campaign based on Ambient Vibration Tests (AVT) to evaluate the modal characteristics of the structure. Subsequently, the Finite Element (FE) model of the church was calibrated to perform the subsequent seismic analysis of the building and identify suitable retrofitting interventions.

A vulnerability index program for steel structures has been developed by Amellal, Bensaibi [20] and Mahmoud [21] considering several parameters. Focusing on reinforced concrete (RC) structures, Hans, Boutin [22] studied the results of in-situ measurements and their interest for a seismic assessment of existing buildings. The response to ambient vibrations, harmonic excitation and shock loading was recorded and the advantages from each technique for the vulnerability assessment of existing buildings were discussed. Michel, Guéguen [23] deepened the use of frequency domain decomposition for modal analysis to identify the building stiffness. A nine-story RC dwelling was finally used to compare the building motion deduced from the numerical model estimated using ambient vibrations and the recorded real building response. Loh, Chao [24] addressed the issue of structural system identification using earthquake-induced structural response. The proposed methodology was based on the subspace identification algorithm to perform identification of structural dynamic characteristics using input-output seismic response data. A simplified method for the seismic vulnerability assessment of RC buildings is presented by Kassem, Nazri [25] modifying the existing Italian GNDT and the European Macro-seismic approaches. Formisano [26] presented usability checks of RC school buildings after the seismic events occurred in Central Italy in 2012, detecting damages and indicating simple straightforward interventions for retrofitting. RC buildings have

been studied in [27,28] through field vibration tests for model updating and to evaluate seismic retrofitting interventions. Seismic upgrading and retrofitting of existing buildings have been also deepen in [29,30].

Numerical tools for vulnerability assessment have been developed by El Khoudri, Ben Allal [31] studying the use of incremental dynamic analysis and pushover analysis as appropriate tool to predict the distribution of expected losses due to earthquake shaking. Later on, an improved method to assess the seismic vulnerability of buildings in urban areas is proposed by Ródenas, García-Ayllón [32] in order to advance the management of seismic emergency scenarios. The methodology gives continuity to the different RISK-UE published works and, when combined with Geographic Information System (GIS), may provide valuable information to manage post-earthquake emergency situations.

Large scale evaluation of community response in case of disastrous earthquake events has been also developed in literature for the assessment of seismic resilience, damage, losses, emergency evacuation and recovering operations [33-36].

Recently, a new Italian standard [4] introduced a guideline to compute the seismic vulnerability index for existing buildings based on the maximum bearable seismic action. Furthermore, it uses the Ultimate Limit State (ULS) earthquake intensity that should be used to design a new building with the same characteristics of the existing one as a reference measure. However, current Italian standard [4] does not provide any specific procedure which to be followed for analysis and computation of maximum bearing capacity. It can be interpreted as an implicit recognition of the singularity of each structure that comes from different designs and uncertainties. Therefore, a methodology that combines specific processes, e.g. field testing and numerical modeling, to compute a reasonable vulnerability index with the purpose of being replicated on a large number of buildings is still lacking.

In this work, an integrated approach for the seismic vulnerability assessment of existing buildings is proposed and applied to an existing RC school in North Italy. The method includes a preliminary analysis

of the building and a survey using nondestructive methods. Subsequently, dynamic modal characteristics are identified to calibrate numerical FE models and perform seismic nonlinear analysis. Finally, different options for the vulnerability index computation are discussed.

Underlining the innovative aspects of the present research, they consist in: (i) real-time data acquisition and structural health monitoring (SHM) using different wireless sensors, i.e. MEMS and force-balance; (ii) alternative dynamic identification methods, such as output-only or forced-vibrations ones. Furthermore, (iii) different formulations for the vulnerability index computation are proposed and compared together. Besides, (iv) the aspects related to the interaction between adjacent buildings (hammering impact) are also discussed.

Next section provides a description of the methodology that has been followed to develop the present work. Subsequently, the description of the field investigations and the data processing for modal characteristics identification is provided, along with the application of the procedure to an existing school building. The final steps of the present study consist in (i) the finite element model development and validation of the existing structure for the subsequent (ii) vulnerability assessment. Finally, different formulations to compute vulnerability indices have been proposed and evaluated on the school building case study.

2. METHODOLOGY FOR SEISMIC VULNERABILITY

This research moves from the identification of a reliable methodology that could be employed to perform the seismic vulnerability assessment of existing buildings. With this aim, a preliminary step consists in the field investigations that include both static and dynamic tests to calibrate further FE procedures for the numerical analysis.

The field investigations start with a survey of the original design documentation. This step can be critical because design tables and reports are often not available, even for governmental and public buildings. In this case, an inspection would be necessary with the preparation of a new geometric and informative model of the building. The survey of experts able to detect possible deterioration conditions, structural and non-structural peculiarities, and materials characteristics represents the next step. Finally, the field investigations are completed by the dynamic measurements and the identification of the modal characteristics through consolidated *output-only* numerical procedures. In parallel, the use of forced vibrations techniques for dynamic identification is also considered using the eccentric mass shaker (vibrodyne) with potential interaction effects between different building's modules (hammering).

Finally, the numerical model of the existing building is prepared and validated against the identified modal characteristics. The structural nonlinear behavior is also modeled to include the post-elastic response in the numerical analyses. The seismic vulnerability assessment is completed by computing the vulnerability index through different approaches with reference to the standard requirements.

A case study of an existing school building in the northern Italy is also adopted to evaluate in detail the proposed procedure on a real test-bed. It is characterized by some specific aspects that can be met frequently in existing buildings: the age of construction ('60s), the design with outdated standards, the use of reinforced concrete for the frames, the presence of structural joints that can origin hammering phenomena.

3. FIELD INVESTIGATIONS

The first step consists in the *historical-critical analysis* to collect all available documents (calculations book, material test certificates, etc.) that reflect the origin and transformation phases to the actual building condition.

Novel techniques have been developed to archive construction data. For instance, Building Information Modeling (BIM) allows implementing a comprehensive database about all different aspects related to a construction process. However, BIM models rarely contain detailed design information that can be used to create a structural FE model able to reproduce the real behavior of existing buildings. Therefore, an accurate *geometric-structural survey* has to be performed to understand the geometry and construction details together with constitutive materials' characterization.

3.1 Non-destructive tests

The available methods are basically classified as *destructive* (direct) and *non-destructive* tests (indirect). The first ones are strength tests as concrete compression test or tensile test on steel reinforcing bars. They can be carried out directly on specimens obtained from concrete core drilling on the existing structure or steel reinforcements extracted from existing structural elements. On the other hand, non-destructive tests involve the indirect measurements of constitutive properties directly measuring certain physical or chemical characteristics through empirical or mathematical correlations. For example, a pachometer can be used to detect the presence of ferromagnetic materials (e.g. steel and iron) embedded in concrete. It is also used to determine the thickness of the concrete cover over the steel reinforcement. The pachometer operates by generating a magnetic field and measuring the reaction between the magnetic field and the metal. The intensity of the response is then related to the location and size of the embedded material.

Another device that is commonly used is the concrete test hammer or sclerometer to measure the concrete compression strength. The device measures the rebound value and through conversion tables the value of the compressive strength can be determined. Thermal camera is also used to detect structural elements that were not reported in the available technical drawings or BIM model. The device is an infrared camera able to detect the different degrees of irradiation emitted by the different surface materials.

3.2 Dynamic characterization

System identification is defined as the preparation of a model based on experimental measurements that can be used to calibrate the initial FE model or utilized in a global SHM to detect the presence, location, and amount of deterioration within the structure [37]. Monitoring schemes are basically used in earthquake engineering and dynamics of structures to identify natural frequencies, modal shapes and damping coefficients of structures, through identification algorithms. Structural identification methods are classified as *analytical*, *experimental* and *operational* approaches.

Analytical approaches determine modal parameters by solving an eigenvalues problem knowing the system characteristics such as geometry, constraints, materials' properties, masses' distribution, stiffness and damping. With reference to *experimental* approaches, starting from measurements of the dynamic input and structural response, frequency response functions (FRF) are computed and the dynamic structural characteristics are identified using the experimental modal analysis (EMA or input-output method). On the contrary, *operational* approaches assess the dynamic parameters only through the structural response without knowing the input excitation, using the operational modal analysis (OMA or *output-only* method). Such identification technique can successfully perform when the response of the structural system is independent of the input, or in other words, when the transfer function of the system is independent of the external loading. It is usually related to stationary (or weakly stationary) white signals [38].

Over the last three decades, substantial progress has been made in input-output methods. However, EMA techniques are not feasible and practical for large structures because it requires the application of a known input with high intensity to excite the entire structure. Instead, OMA methods use ambient noise, avoiding the use of expensive instrumentation to excite the structure. In the following, the most used identification techniques, for both input-output and output-only methods, are summarized.

3.2.1 Frequency Response Function (FRF)

The structural response in the frequency domain is defined by the Frequency Response Function (FRF) that contains the information on the dynamic characteristics of the structure. The analysis is based on the use of the Fourier Transform that allows to find the solution of the dynamic equation in the linear range, converting a system of differential equations into a system of algebraic equations:

$$\left(M\omega^2 + C\omega + K\right)\cdot x(\omega) = f(\omega) \tag{1}$$

where ω is circular frequency vector; *M*, *K*, *C* are the mass, rigidity and damping matrices, respectively; $x(\omega)$ and $f(\omega)$ are displacement and loading vectors, respectively. The FRF is evaluated as the ratio between the Fourier Transforms of the response and input:

$$H(j\omega) = \frac{x(j\omega)}{f(j\omega)} \tag{2}$$

where $H(j\omega)$ is the FRF matrix and *j* a complex number [37]. The FRFs are complex functions with real and imaginary part and can be represented also in terms of amplitude and phase by the following equation:

$$\begin{cases} a = \sqrt{\mathrm{Im}^2 + \mathrm{Re}^2} \\ \varphi = \tan^{-1}\left(\dfrac{\mathrm{Im}}{\mathrm{Re}}\right) \end{cases} \tag{3}$$

The FRF real part imaginary assume zero values at the system natural frequencies, while the imaginary part can have positive and negative peaks at the same natural frequencies whose direction is used to determine the associated mode shapes [39].

3.2.2 Frequency Domain Decomposition (FDD)

FDD identification algorithm is based on the Power Spectral Density (PSD) matrix decomposition using the Singular Value Decomposition (SVD). The latter is able to break down the system's spectral response into a set of single degree of freedom systems (SDOF). Therefore, it is possible to estimate the natural modes

with high precision even if the signals are disturbed [40]. The PSD output estimate $\hat{G}_{yy}\left(j\omega\right)$ at discrete frequencies $\omega = \omega_i$ is decomposed by the matrix SVD:

$$\hat{G}_{yy(j\omega)} = U_i S_i U_i^H \tag{4}$$

where $U_i = \left[u_{i1}, u_{i2}, ..., u_{im}\right]$ is an unitary matrix of the singular vectors u_{ij}; and S_i is a diagonal matrix of the singular scalar values S_{ij}. From the graphic representation of singular values spectrum, peaks corresponding to the natural modes can be recognized. Considering the peak related to the k^{th} mode, the corresponding singular vector represents a good approximation of the mode shape $\varphi = u_1$, while the singular value represents the auto-spectral density function of the respective degree of freedom system [41].

3.2.3 Random Decrement Technique (RDT)

RDT is a time domain procedure in which the linear structural response is transformed into a random decrement function. The system response to a random input, at each time instant *t*, consists in three components: (i) the response to an initial displacement, (ii) the response to an initial velocity, and (iii) the response to the random input in the range [*0, t*]. Averaging a high number of time segments of the structural response, the random part of the response will have a tendency to disappear, and the remaining will be the response of the system to the initial conditions [42]. This technique of deriving the impulse response from the response measured under ambient vibration excitation is the RDT. The above discussion is based on a single random response of a structure. To extract the free response of all measured coordinates, the random decrement technique needs to be applied to all the random responses [39].

A further advantage of the time segment averaging method is the noise reduction in the resulting random decrement (RD) functions. On the other hand, application of RD in frequency domain involves estimating the spectral density functions of the system response. The procedure consists of different phases: (i) partitioning of the recorded response signals in different segments, (ii) application of a "window" to reduce

leakage effects, (iii) Discrete Fourier Transform (DFT) computation of "windowed" segments using Fast Fourier Transform (FFT); and (iv) computation of auto-spectral and cross-spectral averages, considering the DFT of the all segments of the recorded data. Finally, the modes can be identified using different modal analysis methods.

3.2.4 Modal Assurance Criterion (MAC)

The Modal Assurance Criterion (MAC) is a general criterion for assessing the degree of consistency (correlation) between two vectors, both real and complex [43-45]. MAC can be used to compare two mode shape vectors φ_r and φ_q. The correlation indicator for the eigenvector of modes q and r is mathematically expressed as:

$$MAC(r,q) = \frac{\left|\{\varphi_r\}^T \{\varphi_q\}\right|^2}{\left(\{\varphi_r\}^T \{\varphi_r\}\right)\left(\{\varphi_q\}^T \{\varphi_q\}\right)} \tag{5}$$

MAC can assume values between 0 and 1; values close to 0 indicate that the mode shapes are not correlated with each other, while values close to the 1 indicate that the modal shapes are fully coherent with each other. Furthermore, MAC can be used to verify if two different identification techniques (e.g., FDD and RDT) estimate the same modal shapes at each frequency. Moreover, it can be used to evaluate FE models, e.g. by estimating the correlation between two modal shapes obtained from experimental tests and FE analysis or from two FE models with different refinement levels. Two mode shapes can be considered compatible if the MAC assumes values higher than 0.8.

3.3 Case study

The methodology is applied to an existing school in the Northern Italy built in 1976. The school is composed of three separated structures: the first one hosts the classrooms, while the other ones are the gym and canteen

buildings (Figure 1). In this paper, the main structure hosting the classrooms is only investigated. It presents a rectangular footprint with dimensions 98.5x20.0 m and a total height of 6.8 m. The structure is divided into three separated blocks by two expansion joints (Figure 2). During the inspection, it was observed that the expansion joints opening consists of about 2.75 cm filled with polystyrene material.

Figure 1. Aerial view of the specimen structures

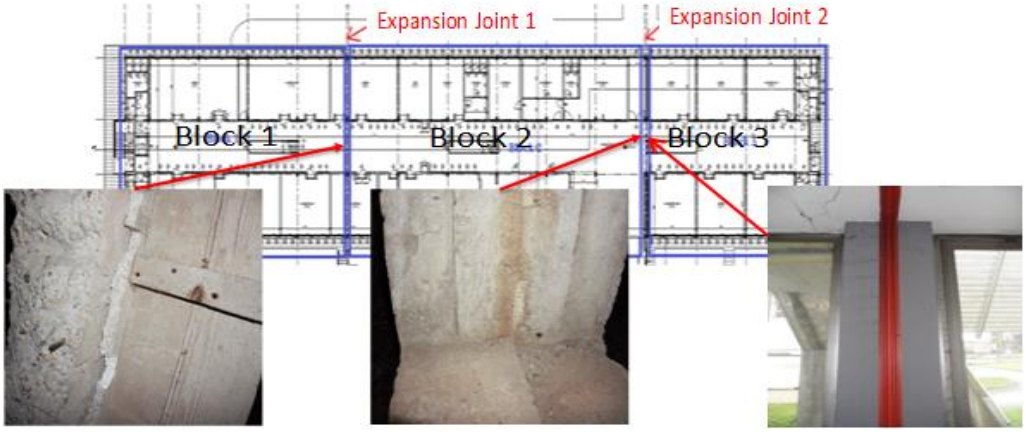

Figure 2. Expansion joints filled with polystyrene material

The original design documents were not available and only few structural data were found on an existing BIM model prepared recently by the municipality. During the field investigation, the building did not show significant cracks or structural damages, while it was possible to observe by visual inspection a limited degradation of concrete surfaces, with spalling and corrosion of the outer reinforcement bars.

3.3.1 Non-destructive tests

A series of non-destructive tests were conducted to obtain the structural parameters such as the concrete module of elasticity and strength, the concrete cover and the steel reinforcements detail in the main structural elements. Tests with thermal camera were also performed to detect structural elements that were not reported in the available technical drawings and BIM model. The device consists in an infrared camera able to detect the different degrees of irradiation emitted by the different surface materials (Figure 3a). Indeed, concrete elements (blue areas) show a lower temperature with respect to the masonry elements, lighting systems and aluminum ventilation shafts (orange and yellow areas).

To identify the material characteristics, a sclerometer test was carried out according to the guidelines provided by the [46] (Figure 3b). Results indicated 31.5 MPa as the average concrete strength for the beams, columns and shear walls. Therefore, the concrete class C25/30 was assumed for the subsequent numerical analyses. Furthermore, a pachometer was used to collect information about spacing, cover and size of steel reinforcement bars inside the concrete elements (Figure 3c). The identified typical column cross section is shown in Figure 3d.

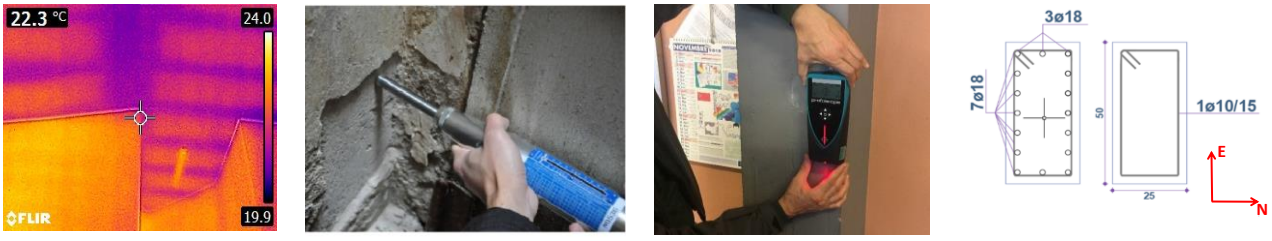

(a) (b) (c) (d)

Figure 3.Thermal camera test (a), sclerometer test (b), pachometer test (c), and column cross section (d)

3.3.2 Dynamic tests

A wireless sensor network was used to collect accelerations at different building positions. The network consisted of five sensing units equipped with MEMS (Micro Electro Mechanical Systems) triaxial

accelerometers (numbered from 50 to 54), and five other sensing units equipped with FB (Force Balance) accelerometers (numbered from 220 to 224).The MEMS sensor is a low noise (7 μg/√Hz) accelerometer with a dynamic range of 90 dB, while the FB one is characterized by a dynamic range of more than 160 dB and a signal-to-noise-ratio lower than 2.5 μg/√Hz.

The units also implemented GPS receivers allowing to create a local network of synchronized instruments using absolute time, in which one sensor assumes to be the '*Master*' and the others are '*Slaves*'. The Master unit was implemented to communicate with the other ones, collecting data from the Slaves units and coordinate the connection with a remote server. The network can be connected to a PC to manage the data recording, downloading and processing in real time through the remote connection. Figure 4 shows the MEMS and FB accelerometers and their positioning on the building.

(a) (b)

Figure 4. Sensing units with MEMS and FB accelerometers (a) and installation examples (b)

The dynamic characterization of a structure was achieved through ambient vibration and forced vibration tests. The last ones have been performed using a vibrodyne to assess the efficiency of the adopted accelerometers. The vibrodyne was fixed to the RC shear wall connected to elevator containment (Figure 5) at the ground floor level. The device can perform within 0-33 Hz and apply a variable force in the range 0-

40 kN. Different harmonic excitations were applied along the building longitudinal direction (North-South) by varying rotation frequencies from 0 to 30 Hz (corresponding to a varying force of 0 to 40 kN).

Figure 5. Vibrodyne position on the shear wall

Different sensor configurations were considered for dynamic tests. Each one was set individually in each block to verify the efficiency of the expansion joints. Furthermore, the configurations were designed in such a way to record torsional modes characteristics. Four configurations were finally considered for ambient vibration tests (S1A, S2A, S3A and S4A), while for forced vibration tests the sensing units were arranged in V1 and V2 configurations (Figure 6). Each test had duration of about 15 minutes with a sampling frequency fixed at 200Hz.

3.3.3 Identification of modal parameters

Data processing first consists in extrapolation of the raw recorded signals corresponding to each configuration. Then, a low-pass filter is used setting the cut-off frequency at the value of 20Hz. The resulting

signals were processed through FDD and RDT techniques using Matlab codes [47] for ambient vibration tests. The singular values diagram of the PSD matrix as function of frequencies was computed, as well the CPSD matrix through the Cross Power Spectral Density (CPSD) function in Matlab. The graphic representation of the singular spectrum allowed identifying the peaks corresponding to the main natural frequencies.

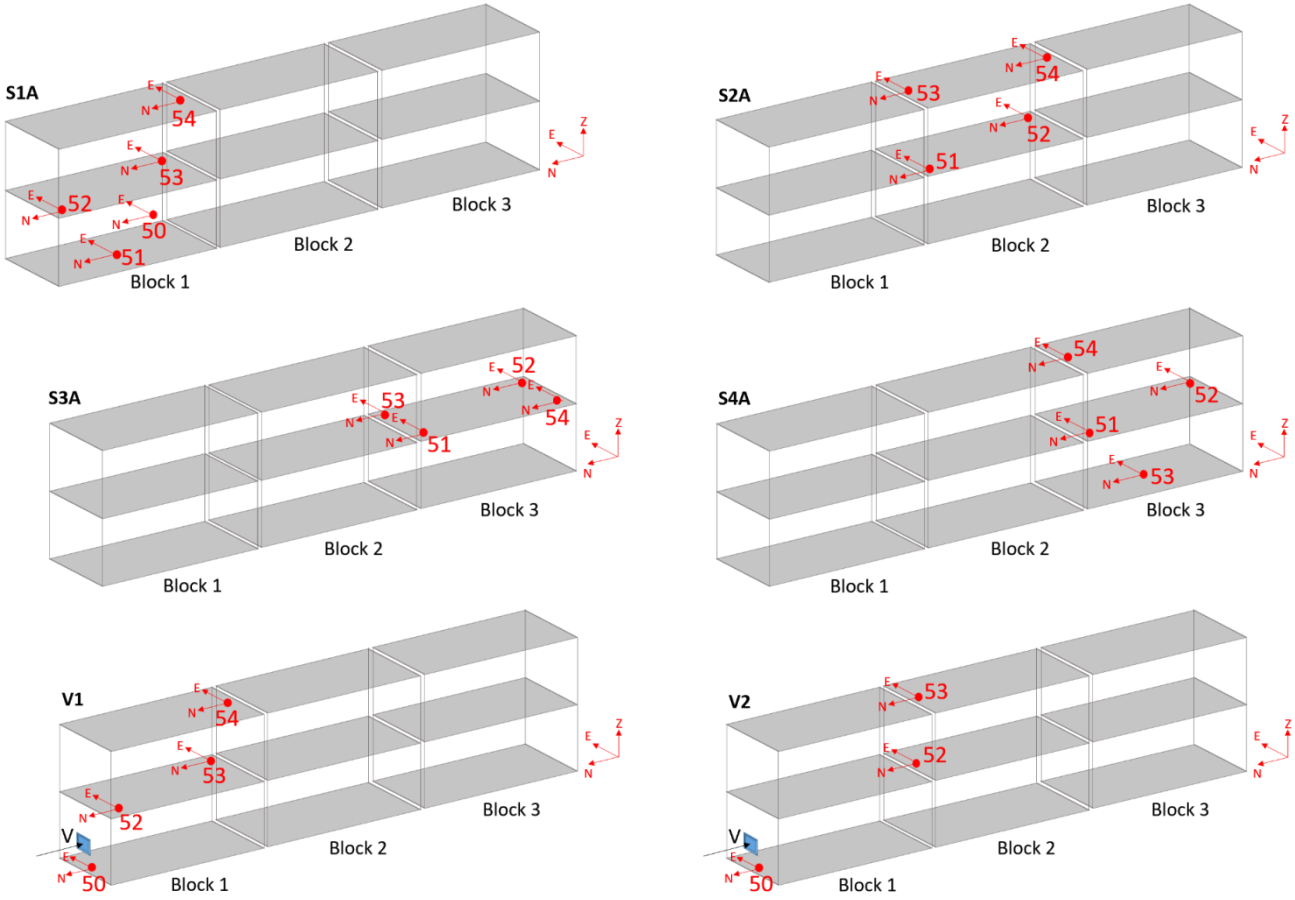

Figure 6. Accelerometer configurations for both ambient and forced vibration tests

An example of the processed signals for the S1A configuration is represented in Figure 7, where the peaks are clearly visible at the same frequency values in both FDD and RDT output-only approaches. In the present case, only FB accelerometers were used as MEMS accelerometers proved to be ineffective to reasonably show the low intensity structural response relative to environmental vibrations only.

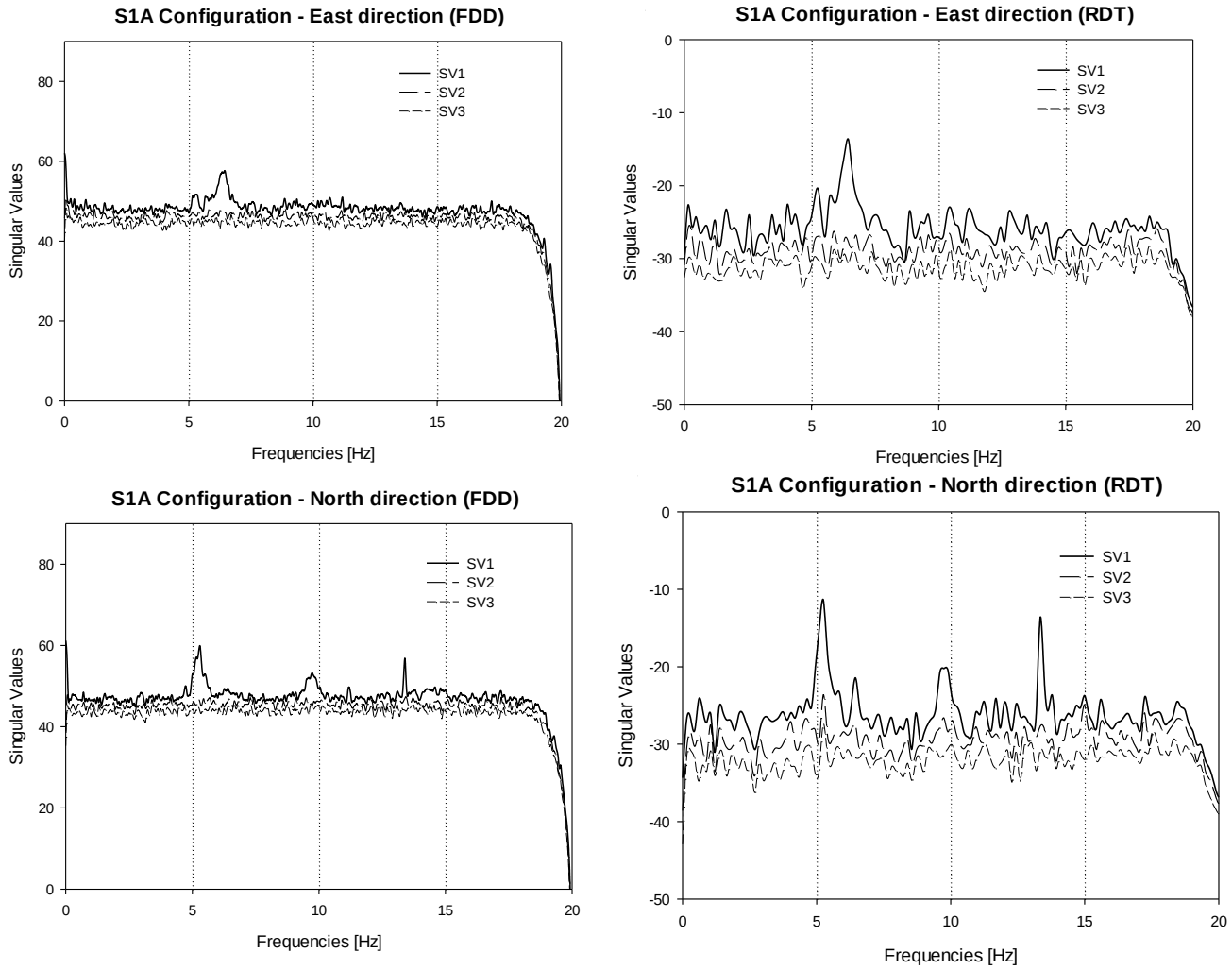

Figure 7. Signal processing using FDD (a) and RDT (b) for configuration S1A in E-W and N-S direction

Table 1 presents the building natural frequencies for Block 1 (S1A configuration). Results indicate: (i) different values in each direction N-S or E-W for flexural modes; (ii) equivalent values in both N-S and E-W directions that can be associated to torsional modes or flexural modes along the diagonal (N-W). As expected, results show that the structure is more rigid in the transversal direction (E-W) since the principal axes of the columns are oriented along this direction (Figure 3 and Figure 6). Furthermore, the identified modes are flexural. The MAC index between the shape vectors FDD and RDT is always higher than 0.8 showing a satisfactory compatibility between the results.

Table 1. Identified natural frequencies for S1A configuration for Block 1

Configuration	Direction	FDD [Hz]	RDT [Hz]	MAC
S1A	E-W	6,45	6,44	0.95
	N-S	5.30	5.24	0.98
		9.75	9.74	0.84
		13.40	13.34	0.99

MEMS recorded data from the vibrodyne tests in N-S direction have been analyzed through the FRF method for V1 and V2 configurations (for Block 1 and Block 2 respectively). A wide range of frequencies from 5 Hz to 30 Hz was applied during the tests (by incrassating 1 Hz at each 30 seconds). In order to measure the input load, an accelerometer (#50) was placed close to the vibrodyne. Normalizing the output with respect to the input in terms of Fourier Transform, the main natural frequencies of the structure were identified. Each FRF was computed and the resonance frequencies were identified where the real part approach zero values. On the other hand, peaks directions of the imaginary part determine the associated mode shapes. Table 2 presents the results for V1 and V2 configurations with respect to those ones computed by output-only techniques for both Block 1 and Block 2.

Table 2. Comparison of natural frequencies between different techniques, Blocks 1 ad 2

Block	Configuration	Direction	FRF [Hz]	FDD [Hz]	RTD [Hz]
1	V1	N-S	5.0	5.3	5.2
			10.0	9.7	9.7
			14.6	13.4	13.3
2	V2	N-S	5.0	5.3	5.4
			10.0	7.3	7.3
			15.0	17.6	17.5

Experimentally, damping coefficients can be estimated through several methodologies including the Half-Power Bandwidth Method (*3dB method*) that uses the amplitude of the peak values of the FRF [48]. Accordingly, the damping ratio has been computed as:

$$\xi = \frac{\omega_2 - \omega_1}{2\omega_0} \tag{6}$$

where ω_1 and ω_2 are the frequencies corresponding to the two half-power points at the resonance frequency (ω_0) [49] . Table 3 reports the identified damping values for V1 and V2 configurations. Three damping values have been calculated for each frequency, where each value corresponds to the damping for each peak and for each accelerometer. To obtain a single damping ratio, the average value was considered.

Table 3. Identified damping and modal shapes for V1 and V2 configuration

Configuration	**Direction**	**Frequency [Hz]**	**Damping at Sensing Units [%]**	**Modal shapes**	**Average Damping [%]**
V1- 1st block	North	5	[1.09 1.02 1.02]	[0.17 0.35 0.55]	1.04
		10	[0.93 0.93 0.93]	[2.06 1.54 1.43]	0.93
		14.61	[3.83 3.73 4.29]	[2.39 3.44 -1.30]	3.95
V2- 2nd block	North	5	[1.16 1.43]	[0.26 0.33]	1.29
		10.04	[1.28 1.28]	[-1.93 -1.49]	1.28
		14.98	[1.28 1.37]	[0.55 -0.32]	1.32

4. FINITE-ELEMENT MODELLING

4.1 Linear models

From the available documentation and the information collected through on-site surveys, a numerical model has been created in SAP2000 [50] and then refined to reproduce the building response. It includes the significant structural elements, and consists of *beam* elements for beams and columns, *gap* elements for infill walls. The gap elements stiffness has been computed using the model of the Equivalent Strut Model

proposed by [51]. All nodes at the base have been fully constrained to reflect the actual conditions. In particular, it was considered appropriate not to model the basement of the classrooms as it consists in a rigid grid of RC beams, and to place the constraints right over them. Furthermore, the presence of joints between the blocks of the classroom building made it possible to model each block separately. During the preliminary stage, an attempt was made to export the model directly from the BIM to the SAP2000 environment but some shortcomings occurred. E.g. lack of materials constitutive parameters, inaccuracy in the definition of beams and columns that responded more to architectural requirements than to structural ones.

The FE models were modeled and calibrated with respect to modal parameters from on-site investigations. For the sake of conciseness, a comparison between different methodologies is reported only for Block 1, as the same level of satisfactory agreement was achieved for the other blocks. Figure 8 shows a qualitative comparison between the mode shapes of Block 1 computed using the FE model and those obtained with FDD methodology. A quantitative comparison is provided by Figure 9. Finally, Table 4 reports the FE computed natural frequencies and those ones obtained by the output-only techniques.

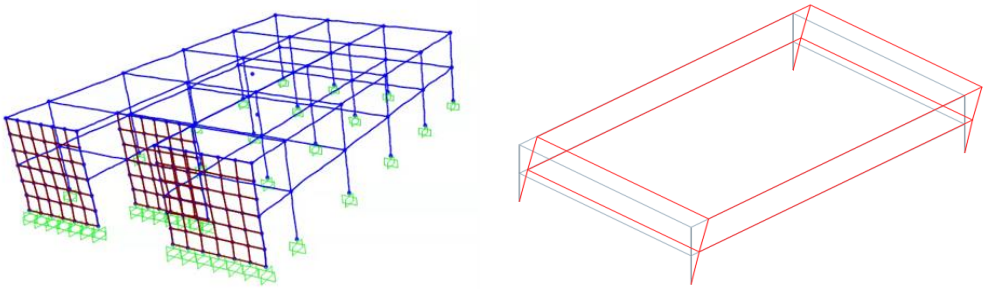

1st mode FE
(a)

1st mode FDD
(b)

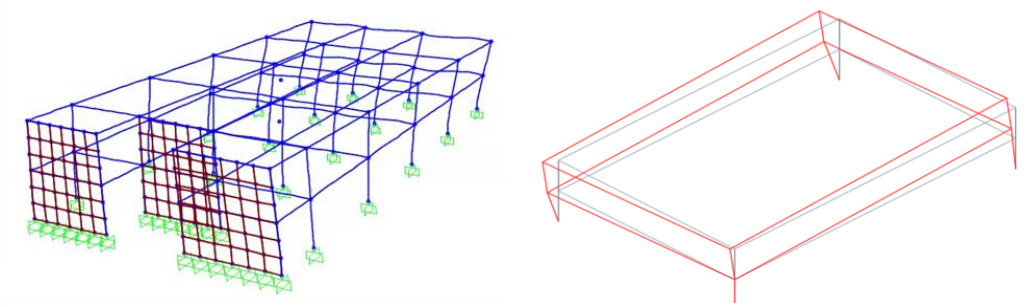

2nd mode FE
(c)

2nd mode FDD
(d)

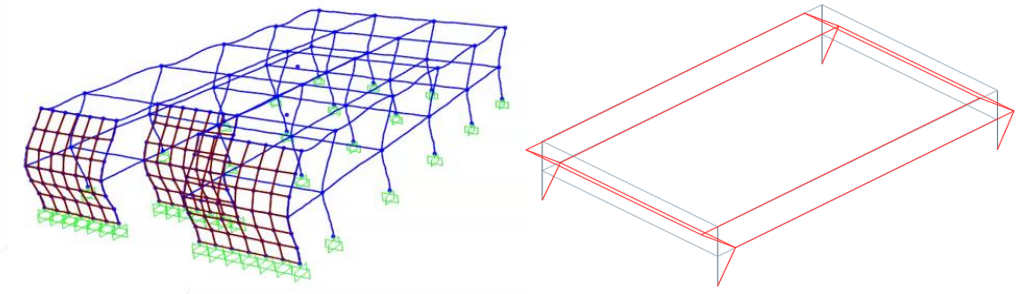

3rd mode FE
(e)

3rd mode FDD
(f)

Figure 8.Qualitative comparison between FEM (a,c,e) and experimental (b,d,f) mode shapes for Block 1

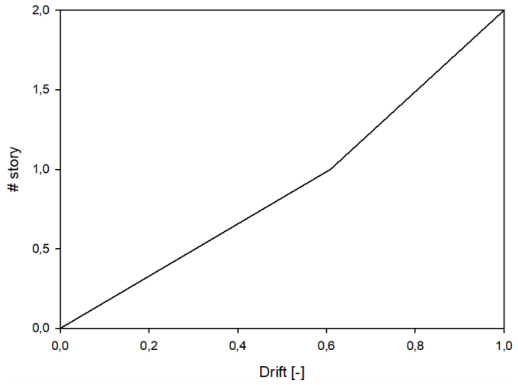

1st mode FE
(a)

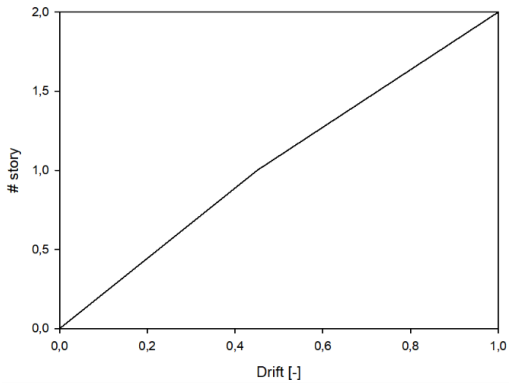

1st mode FDD
(b)

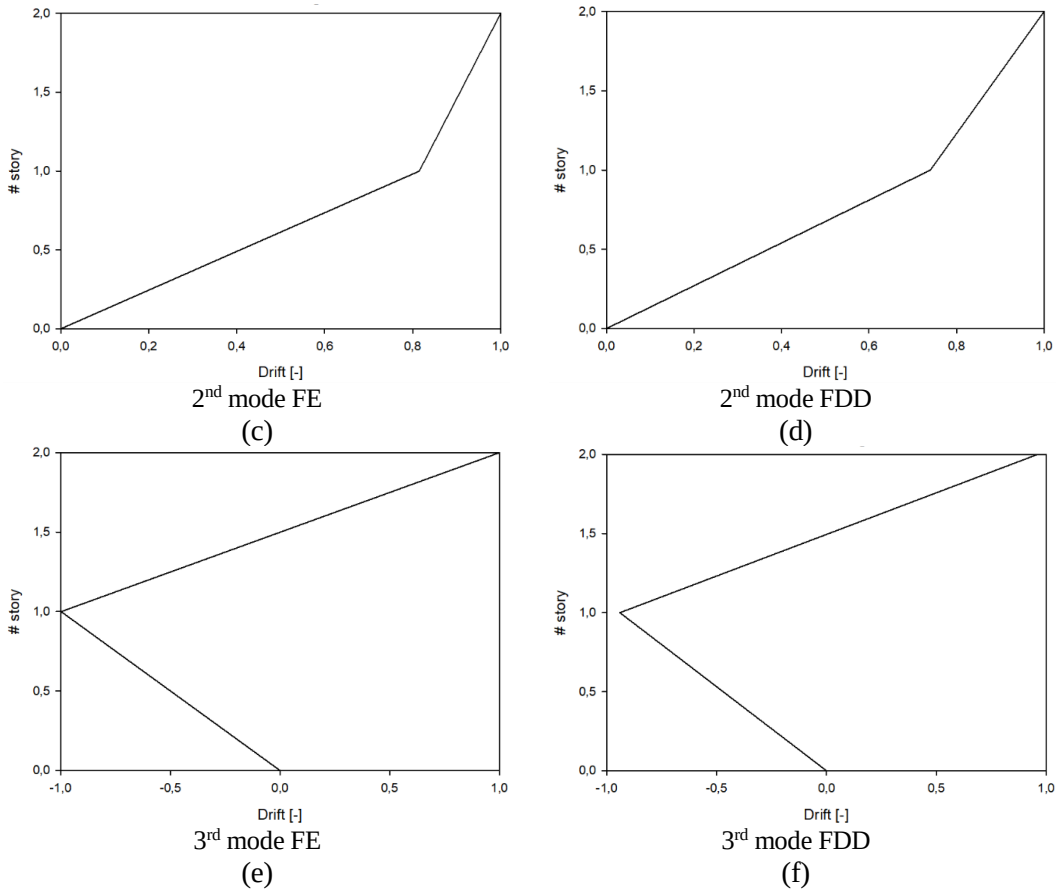

Figure 9.Quantitative comparison between FEM (a,c,e) and experimental (b,d,f) mode shapes for Block 1

Table 4. Comparison between FDD, RDT and FE natural frequencies

	Modes	FDD [Hz]	RDT [Hz]	FE [Hz]	Participation mass ratio
S1A (Block 1)	1st mode	5.33	5.30	5.40	0.91
	2nd mode	6.38	6.50	6.40	0.52
	3rd mode	13.40	13.34	13.20	0.97

4.2 Nonlinear constitutive laws

To assess the seismic vulnerability of the school building, it was necessary to include nonlinearities within the FE numerical models developed in the previous section. With this aim, nonlinear constitutive laws for

construction materials (Figure 10a,b) and plastic hinges [52] were introduced through the adopted FE code. For columns, plastic hinges were assigned for P-M2-M3 degrees of freedom, because of the interaction of bending moments and axial forces, while only for the M3 degree of freedom for beams [50]. Non-linearity for partition walls, on the other hand, was introduced through the *Multilinear Plastic Elements* [50]. To do that, the strength diagram of each type of partition wall was computed on the basis of the *Idealized Force-Deflection Relation* described in FEMA [53]. It is depicted in Figure 10c, where Q is the computed internal force with respect to the expected strength Q_{exp}, Δ_{eff} and h_{eff} are the effective inter-story displacement and height respectively, while d and e are assumed 0.4% and 0.8% of the inter-story displacement, respectively. Parameter c is assumed 0.6% of the expected lateral stress of shear walls and columns. In order to consider the non-linearity of the shear walls, *Layered-Non Linear Shell Elements* have been used [50]. Each element is represented by a surface consisting of several layers (constituted of different materials, i.e. concrete and welded steel mesh) positioned with respect to the reference surface.

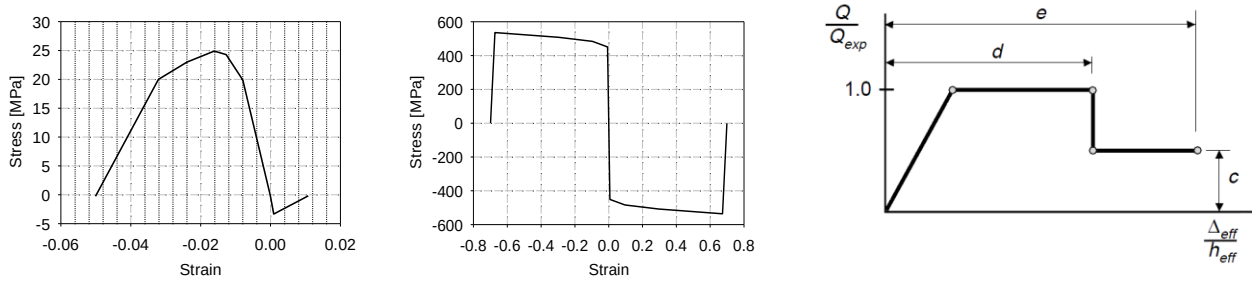

(a) (b) (c)

Figure 10. Concrete (a) and steel (b) stress strain law; idealized force-deflection relation for internal walls (c)

4.3 Contact conditions

To consider possible collapses mechanisms because of hammering effects between adjacent blocks, *gap* elements were defined to model the expansion joints. The gap element is able to connect two adjacent nodes to model the contact conditions. Thus, it reacts with compression interaction forces when adjacent blocks approach each other, while it does not provide tensile forces. The impact compression force is set to be

generated exclusively when the opening parameter (2.75 cm) is exceeded. Figure 11a shows the gap element model with the relevant parameters between connection nodes *i* and *j*. Parameter k is the gap element stiffness that was assumed 10^2-10^4 times the connected elements one.

The gap elements were positioned at the contact nodes of each floor to model potential hammering effects. In that case, all elements may be affected because of internal forces propagation and redistribution, and local or global collapses may also occur. Figure 11b shows the whole FE model with gap elements at the expansion joints. It was employed to perform non-linear dynamic analyses for seismic vulnerability assessment. Figure *12* shows an example of dynamic analysis with gap element activation due to hammering at several time instants. The generation of the contact force at the pounding between the adjacent blocks can be noted.

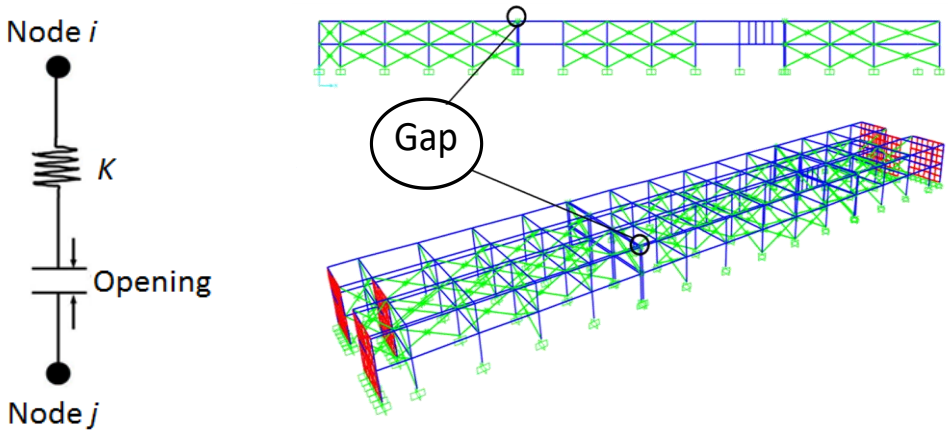

(a) (b)

Figure 11. Gap element model (a) and building FE model with gap elements (b)

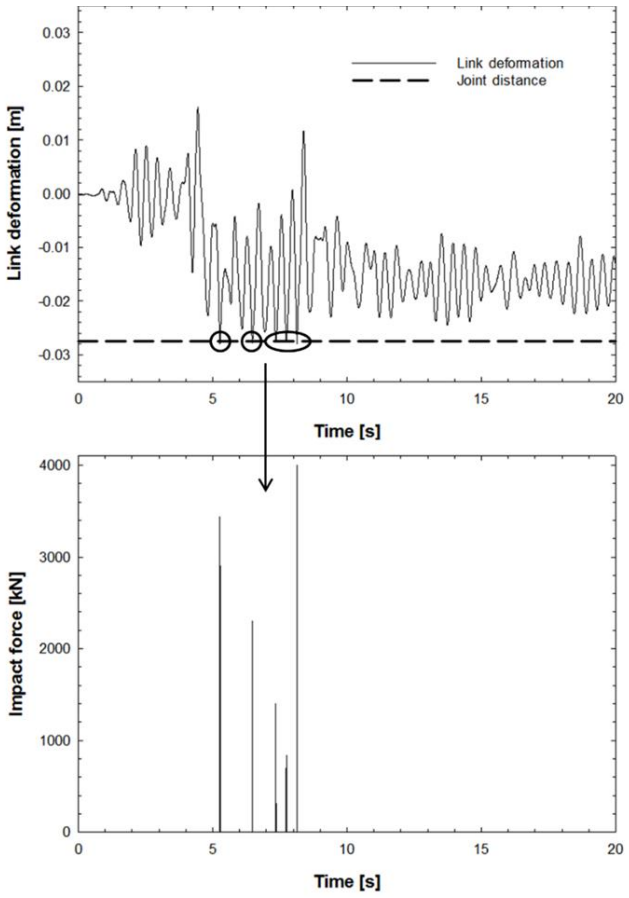

Figure 12. Hammering effect performing nonlinear time history analysis

5. VULNERABILITY ASSESSMENT

The seismic vulnerability of a building depends on the lack of some main features that may affect fundamental structural components. These deficiencies are the consequence of different reasons such as aging, poor maintenance, outdated design, materials' characteristics, the construction place, and natural events. Current Italian standard [4] recommends that the seismic vulnerability assessment of existing buildings, as far as possible, must be carried out in relation to the design guideline for new buildings. To this end, it introduces a new parameter ζ_E as a vulnerability index for a straightforward comparison between the maximum bearable seismic action of the existing structure and that one required to design a new one on the

same soil and with the same vibrational characteristics [54]. The maximum PGA (Peak Ground Acceleration) as a comparison parameter is prescribed.

This section explores the regulatory recommendation (PGA_{max}) in detail and compares it with an alternative formulation to compute the vulnerability index (maximum spectral acceleration at the reference period). Both formulations are presented below and applied to the school building under consideration, composed by three blocks and expansion joints, performing dynamic non-linear analyses.

5.1 Vulnerability index - Method #1

The seismic vulnerability index for existing building introduced by current Italian regulations is based on the following relationship [4]:

$$\zeta_E = \frac{PGA_{Collapse}}{PGA_{Design}} \tag{7}$$

where $PGA_{Collapse}$ is the maximum bearable seismic action of the existing structure in terms of PGA, while PGA_{Design} is the design peak ground acceleration at the Collapse Limit State (CLS) for the new building with the same characteristics of the existing one. Figure 13 summarizes the procedure starting from the field investigations as described in detail for the school building composed of three blocks and two expansion joints. The next main step consists in the 3D finite element model preparation and calibration following the outcomes of the on-site investigations. The nonlinear characteristics have to be introduced in order to reproduce the potential collapse mechanisms. For the school building they are related to the potential generation of plastic hinges at the main structural components of the RC frame and hammering phenomena. To define the maximum bearable seismic action PGA_{Design} at Equation 7, an iterative procedure at is used. To this aim, seven SLC spectrum compatible records were selected in both horizontal directions using the GMSM (Ground Motion Selection Modification) procedure based on the seismic energy principle [55]. The

selected records are compatible with the spectral acceleration at the reference period of structure (0.19 s) and with the seismogenetic parameters of the site. Furthermore, OpenSignal software [56] was used to select the seven records.

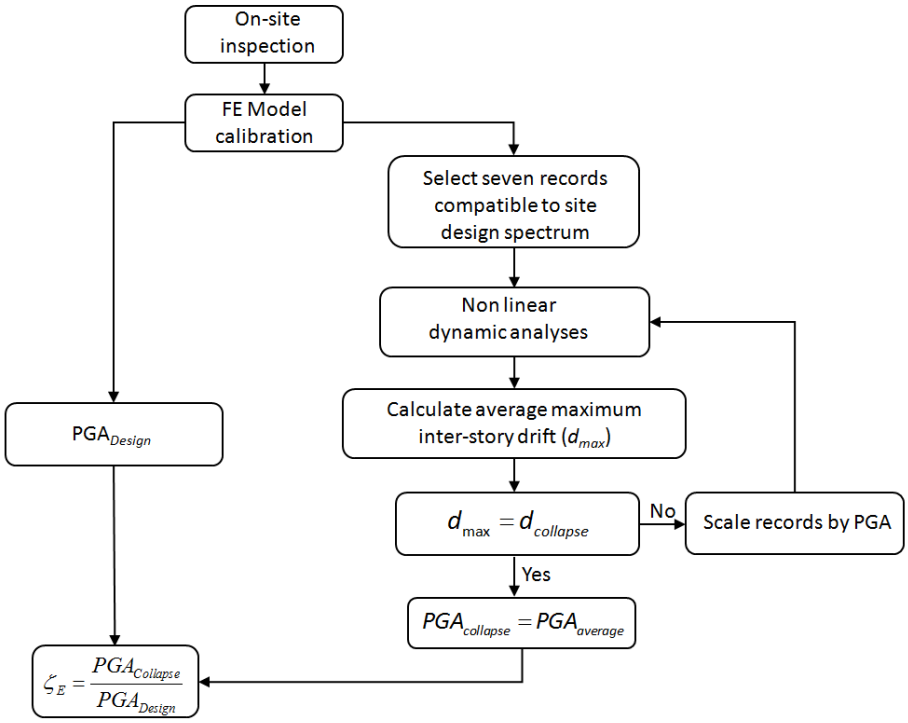

Figure 13. Flowchart for the vulnerability index computation with Method #1

Dynamic nonlinear analyses were performed by applying accelerations in both directions simultaneously. According to FEMA [53], the maximum inter-story drift associated to the collapse prevention limit state for buildings with shear walls in both directions is set as 2% (for Block 1 and Block 3), while for framed buildings it is defined as 4% (for Block 2). The dynamic response of the building in terms of maximum average inter-story drift was calculated for the seven time histories and compared with the maximum allowable inter-story displacement representative of the collapse prevention limit state (CP). If the computed drift was lower than the target displacement, the records were scaled based on PGA until the average of the

maximum inter-story drift for all seven records reached the target. At this iteration, $PGA_{Collapse}$ value was identified as the average of the PGAs of the seven records.

Figure 14 illustrates the spectra of the seven selected records and the mean spectrum compatible with the site spectrum, for both horizontal directions. The target drift was reached firstly at Block 1 (2% of drift), while the second one was more flexible with respect to the other ones (Figure 15). Furthermore, Block 3 reached 1.7% showing more strength with respect to the first one. Finally, $PGA_{Collapse}$ (average value of PGA of seven final scaled records) resulted 0.337 g, while the vulnerability index equals to 1.57 (Table 5).

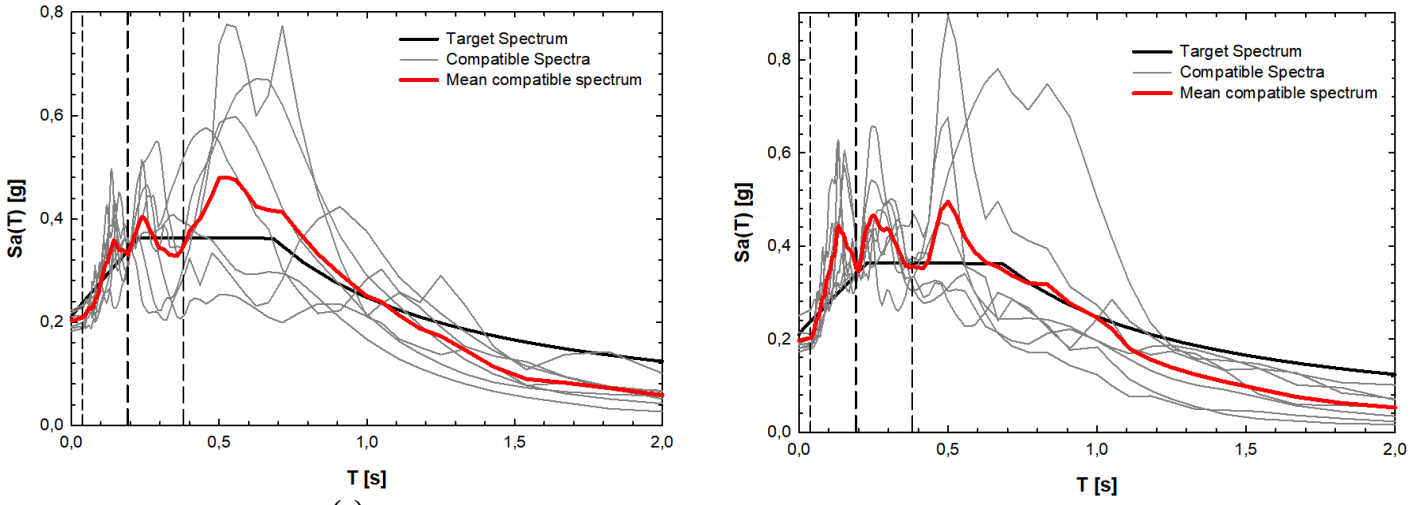

(a) (b)

Figure 14. Input spectra at collapse: (a) x and (b) y direction

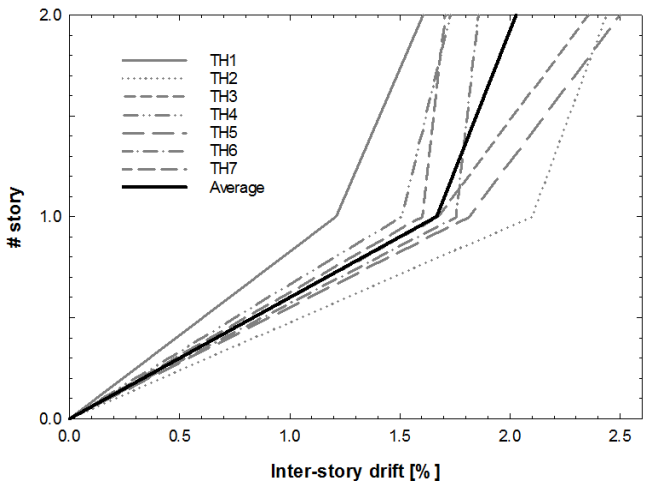

(a)

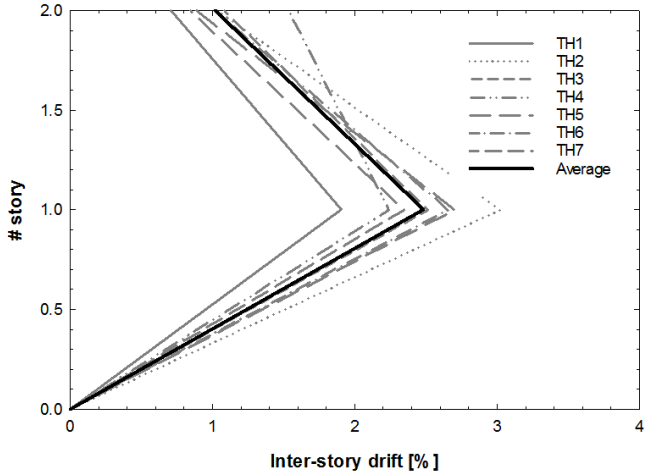

(b)

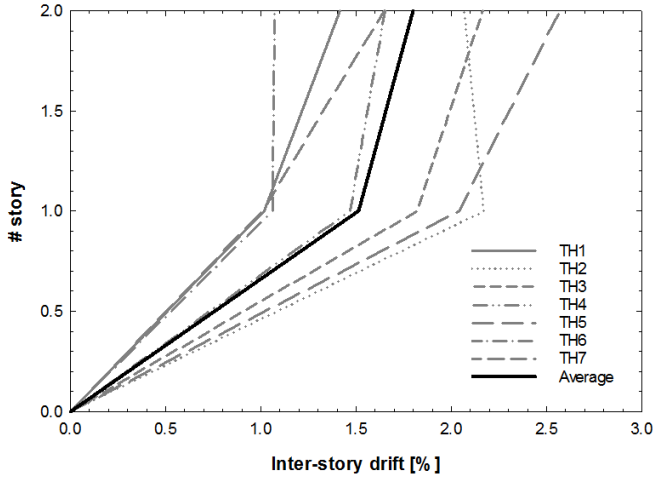

(c)

Figure 15. Inter-story drift related to collapse prevention limit for Block 1 (a), Block 2 (b) and Block 3 (c) using Method #1

Table 5. Vulnerability index evaluated using Method #1

PGA_{Design} [g]	$PGA_{Collapse}$ [g]	ζ_E
0.214	0.337	1,57

5.2 Vulnerability index - Method #2

An alternative formulation to compute the vulnerability index (ζ'_E) is proposed as follows:

$$\zeta'_E = \frac{S_a}{S_d} \tag{8}$$

where S_a is the maximum bearable spectral acceleration of the existing building at the reference period of the structure, while S_d is the CLS spectral acceleration that would be used in the design of a new building on the same soil, with the same characteristics, at the reference period. The new vulnerability index can be computed following Figure 16. In this method with respect to the first one, the spectral acceleration at the reference period is considered as critical parameter instead of PGA.

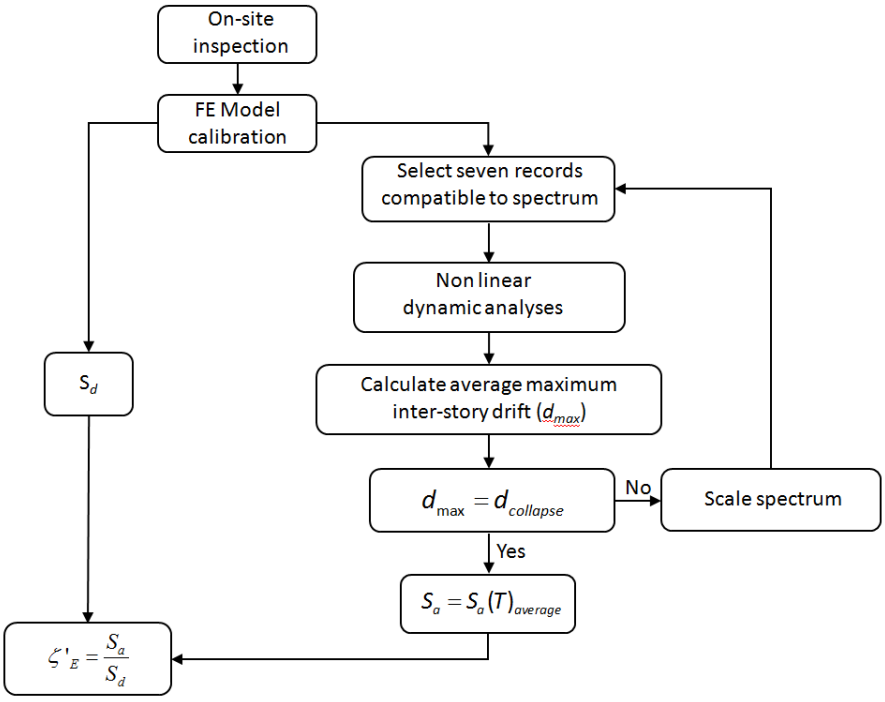

Figure 16. Flowchart to compute the vulnerability index with Method #2

The spectral acceleration at the denominator of Equation 8 (S_d) is fixed by the design spectrum at site considering the first natural period of the existing building. For the school under study, it resulted 0.332 g at the reference period of 0.19s (Figure 14).

Spectral acceleration Sa, representing the collapse state, is defined through dynamic non-linear analyses by iteratively scaling the site design spectrum. Thus, at each step seven records compatible with the scaled spectrum are selected. Coherently with Method #1, time histories were applied simultaneously in both horizontal directions and inter-story drift limits were used to identify the target spectral acceleration: i.e. 2% for blocks with shear walls (Block 1 and Block 3) and 4% for framed building (Block 2).

For each set of time histories, the dynamic response (in terms of maximum average inter-story drift) was computed and compared with the inter-story drift representative of the collapse prevention (CP) limit state. Differently for the previous Method #1, if the calculated inter-story drift was lower than the one corresponding to collapse, a new set of records is selected based on the scaled design spectrum. This procedure is repeated until the average of the maximum inter-story drift values for seven time histories reaches the drift value corresponding to the CP limit.

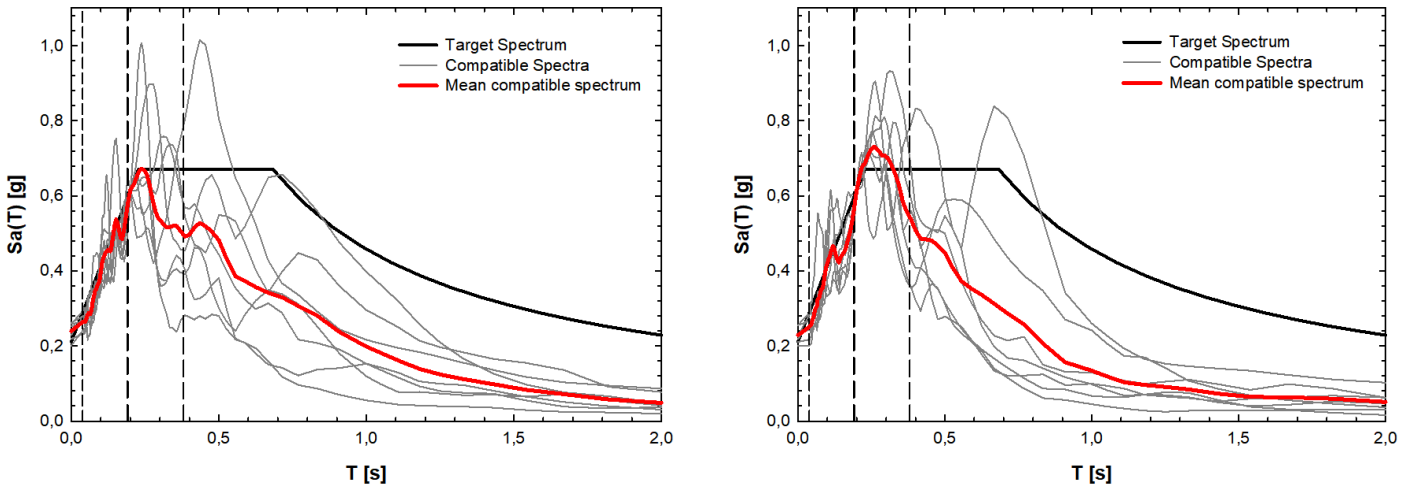

Figure 17. Target spectra at collapse: x direction (a) and y direction (b)

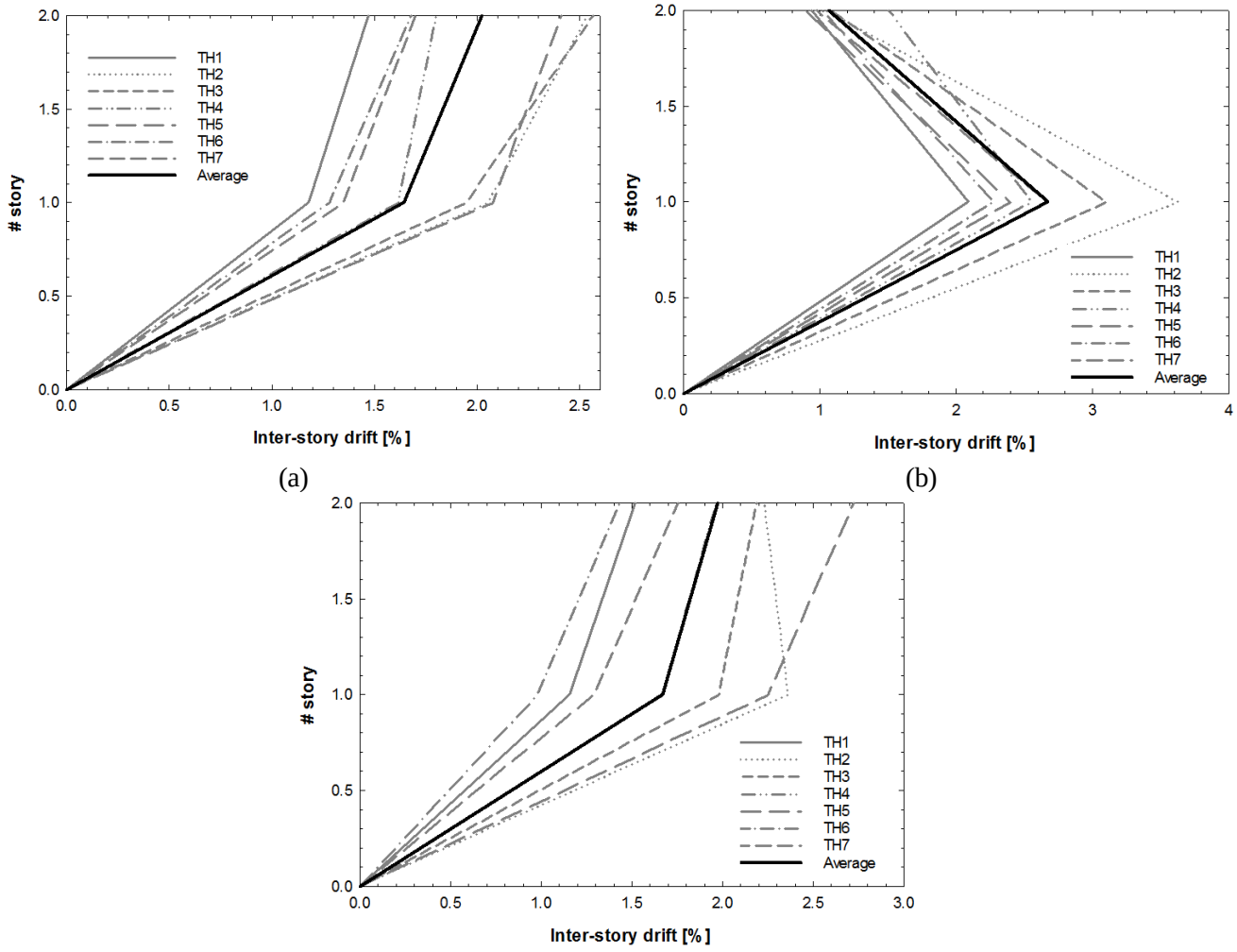

Figure 18. Inter-story drift related to collapse prevention limit for Block 1 (a), Block 2 (b) and Block 3 (c) using Method #2

With respect to Method #1, this method is more accurate but less immediate because at each iteration step it is necessary to amplify the reference spectrum and then to select a new compatible set of records.

For the school building, spectral acceleration S_a was computed as the maximum bearable spectral acceleration corresponding to the earliest achievement of the CP limit drift in one of the three blocks. Figure 17 shows the target spectra at collapse and the mean spectrum of seven compatible records, for both horizontal directions. The block that collapsed first is Block 1 with an average inter-story drift of 2%, while

the second and third blocks reached 2.7% and 1.8%, respectively (Figure 18). Finally, S_a resulted 0.579 g, and consequently the vulnerability index was calculated as 1.74 (Table 6).

Table 6. Vulnerability index estimated using Method #2

S_d [g]	S_a [g]	ζ'_E
0.332	0.579	1.74

6. DISCUSSION AND CONCLUDING REMARKS

A comprehensive methodology to assess the seismic vulnerability of existing buildings is presented in this paper. It is explained at both theoretical and practical levels by adopting an existing school building in the Northern Italy as a test-bed. It consists in a two-story reinforced concrete frame structure with rectangular footprint that assembles three main blocks separated by two structural joints. Shear walls alongside both main directions of the structure are positioned at the building extremities.

The first step of the procedure consists in the on-site investigation to assess the actual structural conditions, to characterize building materials and structural dynamic characteristics. With this aim a wireless sensor network has been used considering two different types of sensors, i.e. MEMS and Force Balance accelerometers. The last ones resulted effective for subsequent application of output-only algorithms for modal identification of the building, which is characterized by a reasonably stiff behavior. On the contrary, MEMS sensors resulted effective exclusively for forced vibration tests employing a vibrodyne to input harmonic forces.

Different structural identification methods have been implemented to compare and assess their efficiency for dynamic structural characterization. With reference to experimental approaches, frequency response functions have been computed and the modal characteristics have been identified using the experimental modal analysis (input-output method). Besides, operational approaches have been also used within an operational modal analysis scheme (output-only methods). The comparison highlights equivalent results in

terms of modal characterization, however the output only methods resulted more advantageous because they do not require complacencies, as the use of vibrodyne, apart low noise sensing units with reasonable dynamic range and resolution. Furthermore, the employed wireless sensor network presents essential advantages with respect to the traditional equipment because it allows avoiding wire coils handling and complicated connections.

The second main step of the procedure consists in the preparation and validation of a numerical model of the building to reproduce its actual dynamic response in both linear and non-linear domains. A good agreement between the FE model and the structural identification methods in terms of dynamic characteristics has been obtained (differences in terms of modal parameters in the range of 1-2%). In particular, it has been emphasized how the model must be capable of reproducing the potential collapse mechanisms that designate the structural vulnerability. Thus, for the considered school building, a FE model has been implemented adopting nonlinear materials' constitutive laws and the contact interaction at the structural joints. The first ones are associated to the development of local and global mechanisms because of plastic hinges formation, while the second ones to hammering phenomena. Neglecting one of these characteristics in building modeling would not allow to evaluate all possible collapse mechanisms and therefore would significantly affect the estimation of vulnerability.

Finally, the seismic vulnerability index as recently introduced by the Italian standard (Method #1) has been compared with a new formulation herein presented (Method #2). Both indices make reference to the design guideline for new buildings. However, they differ for the reference parameter, which is the peak ground acceleration (Method #1), while the proposed formula refers to the spectral acceleration (Method #2). For the school building application herein considered, Method #1 resulted more conservative in terms of vulnerability index (10% smaller) with respect to Method #2.

Method #2 is less immediate because at each iteration up to the collapse the target spectrum has to be amplified and a new compatible set of records to be selected. However, Method #2 can be considered more accurate, indeed the average spectrum recomputed at each iteration matches better the target spectrum at the reference period, with respect to Method #1.

ACKNOWLEDGEMENTS

The research leading to these results has received funding from the European Research Council under the Grant Agreement n° ERC_IDEAL RESCUE_637842 of the project IDEAL RESCUE - Integrated Design and Control of Sustainable Communities during Emergencies. Furthermore, the authors would like to thank the Municipality to which the school building belongs and Dr. Valentina Villa (Politecnico di Torino) for their endless supports and providing the BIM model. Prof. Farhad Ansari (University of Illinois at Chicago) is gratefully acknowledged for his expert support to the on-site investigations and his helpful suggestions. Prof. Fabio Casciati (University of Pavia) is also gratefully acknowledged for allowing vibrodyne to be made available. The cooperation of the doctoral students and post-docs of the Resilience Lab at the Politecnico di Torino – DISEG for the on-site investigations is also acknowledged.

REFERENCES

[1] D.M. Norme tecniche aggiornate relative all'edilizia scolastica. Updated technical standards for school buildings, Italy. Gazzetta Ufficiale 18 Dicembre 1975.

[2] Legge. Provvedimenti per le costruzioni con particolari prescrizioni per le zone sismiche. Measures for buildings with special requirements for seismic areas, Italy. Gazzetta Ufficiale 2 Febbraio 1974 n.64.

[3] Pinto MR. L'osservatorio e l'anagrafe dell'edilizia scolastica per la programmazione della manutenzione. TECHNE: Journal of Technology for Architecture & Environment 2015;9.

[4] D.M. Aggiornamento delle Norme Tecniche per le Costruzioni. Updating of the Technical standards for construction, Italy. Gazzetta Ufficiale 17 Gennaio 2018.

[5] Naeim F, Bhatia H, Lobo RM. Performance based seismic engineering. The Seismic Design Handbook: Springer; 2001. p. 757-92.

[6] D.M. Norme tecniche per la progettazione e la costruzione degli sbarramenti di ritenuta (dighe e traverse). Technical guidelines for the design and construction of dams, Italy. Gazzetta Ufficiale 26 Giugno 2014.

[7] Colombo M, Domaneschi M, Ghisi A, Griffini S. Bearable maximum seismic action for existing concrete dams. 2018.

[8] Calvi GM, Pinho R, Magenes G, Bommer JJ, Restrepo-Vélez LF, Crowley H. Development of seismic vulnerability assessment methodologies over the past 30 years. ISET journal of Earthquake Technology 2006;43:75-104.

[9] Colombini S. Vulnerabilità sismica di edifici esistenti in cemento armato e in muratura. Roma: EPC Editore 2014.

[10] Chácara C, Cannizzaro F, Pantò B, Caliò I, Lourenço PB. Seismic vulnerability of URM structures based on a Discrete Macro-Element Modeling (DMEM) approach. Engineering Structures 2019;201:109715.

[11] Khan SU, Qureshi MI, Rana IA, Maqsoom A. An empirical relationship between seismic risk perception and physical vulnerability: a case study of Malakand, Pakistan. International Journal of Disaster Risk Reduction 2019;41:101317.

[12] Lorenzoni F, Valluzzi MR, Modena C. Seismic assessment and numerical modelling of the Sarno Baths, Pompeii. Journal of Cultural Heritage 2019;40:288-98.

[13] Djemai M, Bensaibi M, Zellat K. Seismic vulnerability assessment of bridges using analytical hierarchy process. IOP Conference Series: Materials Science and Engineering: IOP Publishing; 2019. p. 012106.

[14] Chieffo N, Clementi F, Formisano A, Lenci S. Comparative fragility methods for seismic assessment of masonry buildings located in Muccia (Italy). Journal of Building Engineering 2019:100813.

[15] Gentile R, Galasso C, Idris Y, Rusydy I, Meilianda E. From rapid visual survey to multi-hazard risk prioritisation and numerical fragility of school buildings. Natural Hazards and Earth System Sciences Discussions 2019;19:1365-86.

[16] Giordano N, De Luca F, Sextos A. Out-of-plane closed-form solution for the seismic assessment of unreinforced masonry schools in Nepal. Engineering Structures 2020;203:109548.

[17] Asteris PG, Chronopoulos M, Chrysostomou C, Varum H, Plevris V, Kyriakides N, et al. Seismic vulnerability assessment of historical masonry structural systems. Engineering Structures 2014;62:118-34.

[18] Formisano A, Marzo A. Simplified and refined methods for seismic vulnerability assessment and retrofitting of an Italian cultural heritage masonry building. Computers & Structures 2017;180:13-26.

[19] Di Lorenzo G, Formisano A, Krstevska L, Landolfo R. Ambient vibration test and numerical investigation on the St. Giuliano church in Poggio Picenze (L'aquila, Italy). Journal of Civil Structural Health Monitoring 2019;9:477-90.

[20] Amellal O, Bensaibi M, Grine K. Seismic vulnerability index method for steel structures. Proceedings of the 15th World Conference on Earthquake Engineering (WCEE)2012.

[21] Mahmoud B. Calculation of seismic vulnerability index for steel structures. Energy Procedia 2017;139:558-64.

[22] Hans S, Boutin C, Ibraim E, Roussillon P. In situ experiments and seismic analysis of existing buildings. Part I: Experimental investigations. Earthquake engineering & structural dynamics 2005;34:1513-29.

[23] Michel C, Guéguen P, Bard P-Y. Dynamic parameters of structures extracted from ambient vibration measurements: An aid for the seismic vulnerability assessment of existing buildings in moderate seismic hazard regions. Soil dynamics and earthquake engineering 2008;28:593-604.

[24] Loh CH, Chao SH, Weng JH, Wu TH. Application of subspace identification technique to long-term seismic response monitoring of structures. Earthquake Engineering & Structural Dynamics 2015;44:385-402.

[25] Kassem MM, Nazri FM, Farsangi EN. Development of seismic vulnerability index methodology for reinforced concrete buildings based on nonlinear parametric analyses. MethodsX 2019;6:199-211.

[26 AV1] Formisano A. Seismic damage assessment of school buildings after 2012 Emilia Romagna earthquake. Ingegneria Sismica 2012, 29 (2-3):72-86.

[27 AV2] Soyoz S, Taciroglu E, Orakcal K, Nigbor R, Skolnik D, Lus H, Safak E. Ambient and forced vibration testing of a reinforced concrete building before and after its seismic retrofitting. ASCE Journal of Structural Engineering 2013; 139(10):1741-1752.

[28 AV3] Yu E, Wallace JW, Taciroglu E. Parameter identification of framed structures using an improved finite element model updating method, Part II: Application to experimental data. Earthquake Engineering & Structural Dynamics 2007; 36:641-660.

[29 AV4] Formisano A, Castaldo C, Chiumiento G. Optimal seismic upgrading of a reinforced concrete school building with metal-based devices using an efficient multi-criteria decision-making method. Structure and Infrastructure Engineering 2017; 13(11):1373-1389.

[30 AV5] Formisano A, Iaquinandi A, Mazzolani FM. Seismic retrofitting by FRP of a school building damaged by Emilia-Romagna earthquake. Key Engineering Materials 2015; 624:106-113.

[31 26] El Khoudri M, Ben Allal L, Himi M, El Adak D. Evaluation de la vulnérabilité sismique des bâtiments en béton arméen utilisant l'analyse dynamique incrémentale (Seismic vulnerability assessment of reinforced concrete buildings using Incremental Dynamic Analysis IDA). Journal of Materials and Environmental Science, 2016, vol 7, num 2, p 481-487 2016.

[32 27] Ródenas J, García-Ayllón S, Tomás A. Estimation of the Buildings Seismic Vulnerability: A Methodological Proposal for Planning Ante-Earthquake Scenarios in Urban Areas. Applied Sciences 2018;8:1208.

[33 LS1] Wald D, Lin KW, Porter K, Turner L. ShakeCast: Automating and Improving the Use of ShakeMap for Post-Earthquake Decision-Making and Response. Earthquake Spectra 2008; 24(2): 533-553.

[34 LS2] Lu XZ, Cheng QL, Xu Z, Xu YJ, Sun CJ. Real-time city-scale time-history analysis and its application in resilience-oriented earthquake emergency responses. Applied Sciences 2019; 9(17): 3497.

[35 LS3] Marasco S, Cardoni A, Zamani Noori A, Kammouh O, Domaneschi M, Cimellaro GP. Integrated platform to assess seismic resilience at the community level. Sustainable Cities and Society 2021; 64: art. no. 102506.

[36 LS4] Battegazzorre E, Bottino A, Domaneschi M, Cimellaro GP. IdealCity: A hybrid approach to seismic evacuation modeling. Advances in Engineering Software 2021; 153: art. no. 102956.

[37 28] Cimellaro GP, Piantà S, De Stefano A. Output-only modal identification of ancient L'Aquila city hall and civic tower. Journal of structural engineering 2011;138:481-91.

[38 29] Domaneschi M, Sigurdardottir D, Glisic B. Damage detection on output-only monitoring of dynamic curvature in composite decks. Structural Monitoring and Maintenance 2017;4:1-15.

[39 30] Fu Z-F, He J. Modal analysis: Elsevier; 2001.

[40 31] Brincker R, Zhang L, Andersen P. Modal identification from ambient responses using frequency domain decomposition. Proc of the 18*'International Modal Analysis Conference (IMAC), San Antonio, Texas2000.

[41 32] Brincker R, Zhang L, Andersen P. Modal identification of output-only systems using frequency domain decomposition. Smart materials and structures 2001;10:441.

[42 33] Rodrigues J, Brincker R. Application of the random decrement technique in operational modal analysis. 1st International Operational Modal Analysis Conference: Aalborg Universitet; 2005. p. 191-200.

[43 34] Allemang RJ. The modal assurance criterion–twenty years of use and abuse. Sound and vibration 2003;37:14-23.

[44 35] Pastor M, Binda M, Harčarik T. Modal assurance criterion. Procedia Engineering 2012;48:543-8.

[45 36] Domaneschi M, Martinelli L. Optimal passive and semi-active control of a wind excited suspension bridge. Structure and Infrastructure Engineering 2013;9:242-59.

[46 37] UNI-EN. 12504-2: 2012. Testing concrete in structures Part 2: Non destructive testing-determination of rebounded number 2012.

[47 38] MATLAB. 9.3. 0 (R2017b). The MathWorks Inc, Natick, Massachusetts 2017.

[48 39] Papagiannopoulos GA, Hatzigeorgiou GD. On the use of the half-power bandwidth method to estimate damping in building structures. Soil Dynamics and Earthquake Engineering 2011;31:1075-9.

[49 40] Wang J, Lü D, Jin F, Zhang C. Accuracy of the half-power bandwidth method with a third-order correction for estimating damping in multi-DOF systems. Earthquake Engineering and Engineering Vibration 2013;12:33-8.

[50 41] CSI. Integrated finite element analysis and design of structures basic analysis reference manual. Computers and Structures Inc, Berkeley (CA, USA) 2018.

[51 42] Al-Chaar G. Evaluating strength and stiffness of unreinforced masonry infill structures. US Army Corps of Engineers, Engineer Research and Development Center; 2002.

[52 43] 41-13 AS. Seismic evaluation and retrofit of existing buildings. American Society of Civil Engineers Reston, VA; 2014.

[53 44] FEMA F. NEHRP guidelines for the seismic rehabilitation of buildings. Federal Emergency Management Agency Washnigton, DC; 1997.

[54 45] CIRCOLARE. 21 gennaio 2019, n. 7 CS LL. PP. Istruzioni per l'applicazione dell'Aggiornamento delle "Norme tecniche per le costruzioni", di cui al decreto ministeriale 17 gennaio 2018. 2019.

[55 46] Marasco S, Cimellaro G. A new energy-based ground motion selection and modification method limiting the dynamic response dispersion and preserving the median demand. Bulletin of Earthquake Engineering 2018;16:561-81.

[56 47] Cimellaro GP, Marasco S. A computer-based environment for processing and selection of seismic ground motion records: OPENSIGNAL. Frontiers in Built Environment 2015;1:17.